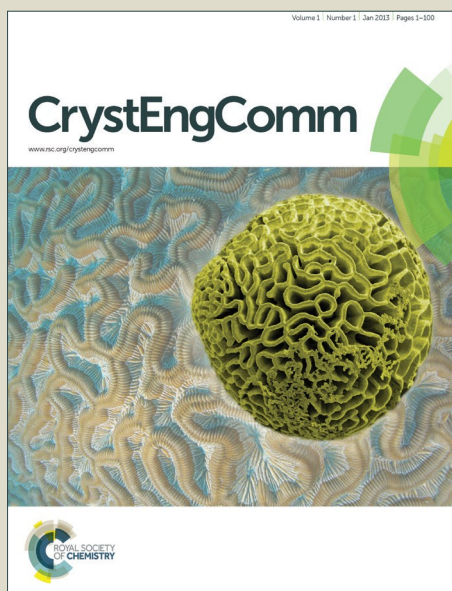


CrystEngComm

Accepted Manuscript



This article can be cited before page numbers have been issued, to do this please use: H. Cui, Y. Wang, Y. Wang, Y. Fan, L. Zhang and C. Su, *CrystEngComm*, 2016, DOI: 10.1039/C6CE00358C.



This is an *Accepted Manuscript*, which has been through the Royal Society of Chemistry peer review process and has been accepted for publication.

Accepted Manuscripts are published online shortly after acceptance, before technical editing, formatting and proof reading. Using this free service, authors can make their results available to the community, in citable form, before we publish the edited article. We will replace this *Accepted Manuscript* with the edited and formatted *Advance Article* as soon as it is available.

You can find more information about *Accepted Manuscripts* in the [Information for Authors](#).

Please note that technical editing may introduce minor changes to the text and/or graphics, which may alter content. The journal's standard [Terms & Conditions](#) and the [Ethical guidelines](#) still apply. In no event shall the Royal Society of Chemistry be held responsible for any errors or omissions in this *Accepted Manuscript* or any consequences arising from the use of any information it contains.

Journal Name

ARTICLE

A Stable and Porous Iridium(III)-Porphyrin Metal-Organic Framework: Synthesis, Structure and Catalysis

Hao Cui,^a Yingxia Wang,^a Yanhu Wang,^a Yanzhong Fan,^a Li Zhang,^{*a} and Cheng-Yong Su^{*ab}Received 00th January 20xx,
Accepted 00th January 20xx

DOI: 10.1039/x0xx00000x

www.rsc.org/

Self-assembly of a new metalloporphyrin tetracarboxylic ligand Ir(TCPP)Cl (TCPP = tetrakis(4-carboxyphenyl)porphyrin) with ZrCl₄ in the presence of benzoic acid leads to the formation of a three-dimensional (3D) iridium(III)-porphyrin metal-organic framework (Ir-PMOF) with the formula of [(Zr₆(μ₃-O)₈(OH)₂(H₂O)₁₀]₂(Ir(TCPP)Cl)₃·solvents (Ir-PMOF-1(Zr)), which possesses square-shaped channels of 1.9 × 1.9 nm² (atom-to-atom distances across opposite Ir metal atoms) in three orthogonal directions as disclosed by the single-crystal X-ray diffraction analysis. Ir-PMOF-1(Zr) represents the first MOF bearing the self-supported iridium-porphyrin catalytic framework, featuring in high porosity and stability. The catalytic tests disclose that the activated Ir-PMOF-1(Zr) can promote O-H insertion with the turnover frequency (TOF) up to 4260 h⁻¹. Ir-PMOF-1(Zr) can be recycled and reused for 10 runs without significant loss of catalytic activity, and the total turnover number (TON) for O-H insertion after 10 successive runs reach 875.

INTRODUCTION

Metal-catalyzed carbene transfer reactions have been widely used for the construction of valuable compounds.¹ Metalloporphyrin complexes of iron,² cobalt,³ ruthenium,⁴ and rhodium,⁵ etc. are known to catalyze olefin cyclopropanation, and further, X-H (X = C, N, Si) bond insertion with high efficiency and selectivity. For example, Rh-porphyrin complexes furnish cyclopropanation and C-H insertion products with unusual selectivity for *cis*-cyclopropanes^{5a} and primary insertion products^{5b}, respectively. Fe- and Ru-porphyrins can catalyze the N-H insertion of ammonia² and peptide containing N-terminal amine,⁴ respectively. Compared to other group 8 and group 9 metals, the reactivity of iridium-porphyrins toward carbene transfer has been much less explored. Recently, intermolecular cyclopropanation and carbene X-H bond insertion have been reported by Woo,⁶ Che⁷ and Rodríguez-García⁸ using Ir-porphyrin catalysts.

Nevertheless, there are two major disadvantages associating with metalloporphyrin catalysis. First, the synthesis

of metalloporphyrin is often challenging and low-yielding. Second, metalloporphyrins are prone to oxidative self-destruction of the catalyst under very strong oxidizing medium. To make better use of metalloporphyrin catalysis, one approach is to immobilize the metalloporphyrin catalyst onto an organic or inorganic polymer.⁹ Immobilization onto a solid support enables the catalysts to be easily recovered and reused, and also reduces the metalloporphyrin degradation. Another alternative immobilization method is to integrate metalloporphyrin onto the backbones of metal-organic frameworks (MOFs).¹⁰ Since MOFs possess uniform, continuous and permeable channels, construction of porous MOFs by using metalloporphyrin ligands can directly install these active sites on the pore surface and facilitate transportation of reactants/products to or from inner reactive vessels. Unlike immobilized metalloporphyrin catalysts onto an organic/inorganic polymer, porphyrinic MOFs lack non-accessible bulk volume and can act as single-site catalysts with 100% utility of active sites.¹¹⁻²⁹

Despite the availability of a large number of porphyrinic MOFs, none of them has embedded iridium-porphyrin complexes as the building blocks, which are known to show catalytic potentials in carbene transfer reactions such as cyclopropanation and N-H insertion.⁶⁻⁸ We have long been working in the field of carbene/nitrene transfer reactions, and are interested to develop efficient while recyclable Ir-porphyrin catalysts to accomplish such catalysis.^{30,31} According to above discussion, we believe that a promising way is to construct iridium(III)-porphyrin metal-organic frameworks (Ir-PMOFs) as the self-supported Ir-porphyrin catalysts. Herein, we report, to the best of our knowledge, the first Ir-porphyrin MOF, Ir-PMOF-1(Zr), which is highly porous and stable, and is

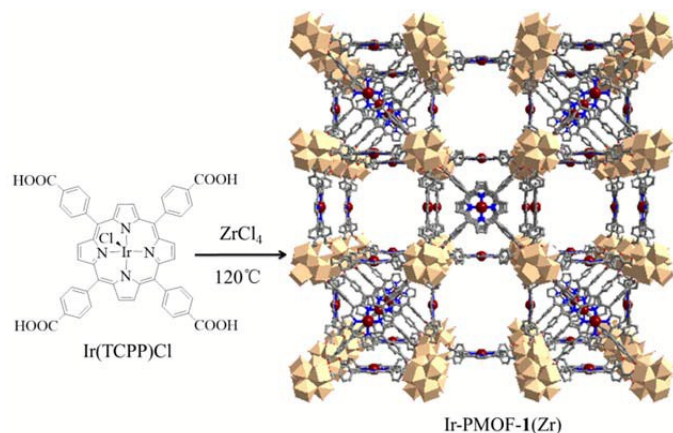
^a MOE Laboratory of Bioinorganic and Synthetic Chemistry, Lehn Institute of Functional Materials, School of Chemistry and Chemical Engineering, Sun Yat-sen University, Guangzhou 510275, China. E-mail: zhli99@mail.sysu.edu.cn; cecscy@mail.sysu.edu.cn

^b State Key Laboratory of Organometallic Chemistry, Shanghai Institute of Organic Chemistry, Chinese Academy of Sciences, Shanghai 200032, China

† Electronic supplementary information (ESI) available: Crystal structure data, physical characterizations, chemical/thermal stability study, and dye adsorption of porphyrinic MOFs, recycling experiments, ICP spectrometric evaluation of metal leaching, and NMR data of O-H insertion products. CIF files giving crystallographic data. CCDC 1436270. For ESI and crystallographic data in CIF or other electronic format see DOI: 10.1039/x0xx00000x.

efficient in the carbenoid insertion reactions into O-H bonds (Scheme 1).

Scheme 1. Ir-PMOF-1(Zr) Synthesis.



EXPERIMENTAL SECTION

General Information. All the reagents in the present work were obtained from the commercial source and used directly without further purification. The ligand 5,10,15,20-tetrakis(4-methoxycarbonylphenyl)porphyrin (TCPPCO₂Me) was synthesized according to the literature.²⁸

Cautions! Although we have not experienced any problem in the handling of the diazo compounds (e.g. ethyl diazoacetate (EDA)), extreme care should be taken when manipulating them due to their explosive nature.

Synthesis of Ir(TCPPCO₂Me)(CO)Cl. Iridium porphyrin complex Ir(TCPPCO₂Me)(CO)Cl was prepared according to a similar procedure.^{7,32} TCPPCO₂Me (100 mg, 11.8 mmol) and [Ir(COD)Cl]₂ (100 mg, 14.9 mmol) in 1,2,4-trichlorobenzene (20 mL) was stirred at 190 °C. After 1 day, the solvent was removed under reduced pressure. The crude reaction mixture was purified on silica using a mixture of DCM and EtOAc as the eluent to afford the product as a red solid (106 mg, 82% yield based on TCPPCO₂Me). ¹H NMR (400 MHz, CDCl₃) δ 8.90 (m, 8 H), 8.46 (m, 8 H), 8.33 (m, 8 H), 4.10 (s, 12 H). ¹³C NMR (100 MHz, CDCl₃) δ 167.33, 145.70, 140.94, 134.70, 134.40, 132.28, 130.30, 128.45, 128.27, 121.60, 52.75. FT-IR (KBr) ν 3428 (br), 2058 (s), 1724 (s), 1607 (s), 1537 (w), 1435 (m), 1401 (w), 1278 (s), 1185 (w), 1111 (s), 1020 (s), 965 (w), 867 (w), 823 (w), 797 (w), 765 (m), 712 (m) cm⁻¹. HRMS (ESI): m/z 1037.2142 [M-CO-Cl]⁺ for [C₅₂H₃₆N₄O₈Ir]⁺ (Calc. 1037.2161). UV-vis (THF, λ_{max}, (log ε)) 419 nm (5.30), 531 nm (4.22).

Synthesis of Ir(TCPP)Cl. Ir(TCPP)Cl was prepared via the hydrolysis of the obtained Ir(TCPPCO₂Me)(CO)Cl according to a similar procedure.²⁸ The obtained ester (120 mg) was stirred in a mixture of THF (6 mL) and MeOH (6 mL), to which a solution of KOH (100 mg) in H₂O (6 mL) was added. This mixture was refluxed for 5 h. After the reaction mixture was cooled down to room temperature, the organic solvents (e.g. THF, MeOH)

were removed under reduced pressure. The crude product as red precipitate was obtained after 1 M HCl was added to the aqueous suspension. Until no further precipitate was detected (pH~2), the crude product was collected, washed with water (60 mL), and dried in vacuum. The yield is 90 mg (81%). ¹H NMR (400 MHz, CD₃OD) δ 8.80 (s, 8 H), 8.44 (d, 2 H, J = 8 Hz), 8.33 (d, 2 H, J = 8 Hz). FT-IR (KBr) ν 3413 (br), 1698 (s), 1605 (s), 1536 (w), 1407 (m), 1355 (m), 1255 (s), 1175 (m), 1102 (m), 1016 (s), 792 (s), 711 (m) cm⁻¹. HRMS (ESI): m/z 981.1522 [M-CO-Cl]⁺ for [C₄₈H₂₈N₄O₈Ir]⁺ (Calc. 981.1534). UV-vis (THF, λ_{max}, (log ε)) 409 nm (5.07), 531 nm (3.96).

Synthesis of [(Zr₆(μ₃-O)₈(OH)₅(H₂O)₇)₂(Ir(TCPP)Cl)₃]-solvents (Ir-PMOF-1(Zr)). Ir(TCPP)Cl (6 mg, 5.9 × 10⁻³ mmol), ZrCl₄ (10 mg, 0.04 mmol), benzoic acid (300 mg, 2.45 mmol) and dimethylformamide (DMF, 1 mL) were placed in a glass vial, which was then sealed and heated to 120 °C in an oven. After 48 h, red block crystals were obtained (6 mg, 64% yield based on Ir(TCPP)Cl) and air-dried. Anal. Calcd. For [(Zr₆(μ₃-O)₈(OH)₂(H₂O)₁₀)₂(Ir(TCPP)Cl)₃]-8(C₆H₅COOH)-4DMF (C₂₁₂H₁₈₉Cl₃Ir₃N₁₆O₈₄Zr₁₂): C, 41.84 H, 3.38; N, 3.69. Found: C, 41.84; H, 3.12; N, 3.57%. FT-IR (KBr) ν 3394 (br), 1601 (s), 1551 (s), 1404 (s), 1015 (m), 718 (m), 652 (m) cm⁻¹.

Single X-ray Crystallography. The X-ray diffraction data was collected with an Agilent Technologies SuperNova X-RAY diffractometer system equipped with Cu-κ α radiation (λ = 1.54178 Å). The crystal was kept at 150.0(1) K during data collection. The structure was solved with the SIR2004 structure solution program integrated in Olex2 using Direct Methods, and refined with the XH refinement package using CGLS minimisation.^{33a} The final refinement was performed by SHELXL-2014/7 (Sheldrick, 2014) imbedded in WINGX.^{33b} The main coordination framework in the crystal lattice show apparent disorder over two closely adjacent positions; however, adequate treatment of this disorder by splitting all atoms into two parts seems troublesome due to high crystal symmetry. Therefore, the refinement was restricted to one set of molecules by using DIFX to constrain porphyrin ligand. ISOR/SIMU was applied to all non-hydrogen atoms to simulate isotropic behaviours. Even though, ADP max/min ratios, especially for Ir and Zr atoms, are not prevented. All solvent molecules have been removed by SQUEEZE program.^{33c} The positions of the hydrogen atoms are generated geometrically. A summary of the crystal structure refinement data and selected bond angles and distances are listed in Table S1 and Table S2.

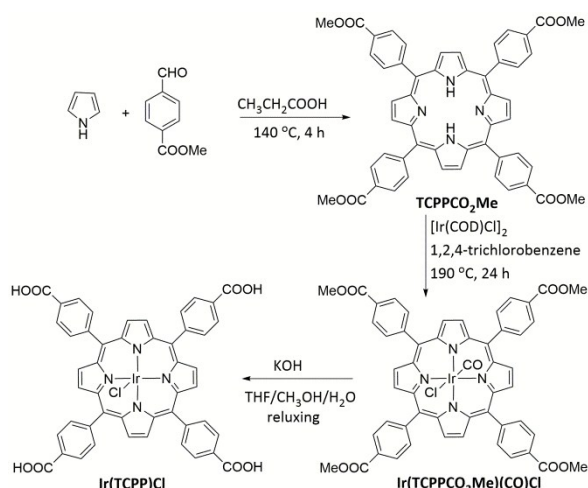
Typical Procedure for O-H Insertion. A solution of EDA (34.2 mg, 0.3 mmol, 1.0 eq) was added slowly to the solution of isopropanol (90 mg, 1.5 mmol, 5.0 eq) and activated Ir-PMOF-1(Zr) (4.7 mg, 0.003 mmol, 1 mol [Ir]%) in DCM (1 mL). The resulting solution was stirred at room temperature for 10 min until EDA was completely consumed. The undissolved catalyst was removed through centrifugation, and washed with DCM (1 mL) and acetone (1 mL × 3). The combined supernatant was evaporated to dryness, and the residue was dissolved in CDCl₃ and analysed by ¹H NMR to determine the conversion of EDA to the alkoxyacetate **2a** (94%). ¹H NMR (400 MHz, CDCl₃) of

2a: δ 4.18 (q, $J = 7.2$ Hz, 2H), 4.03 (s, 2H), 3.68 (m, 1H), 1.25 (t, $J = 7.2$ Hz, 3H), 1.22 (d, $J = 6.1, 1.3$ Hz, 6H).

RESULTS AND DISCUSSION

The general synthesis methods of Ir-porphyrins start from the reaction of $[\text{Ir}(\text{COD})\text{Cl}]_2$ and porphyrin ligands, and offer the product $\text{Ir}(\text{Por})(\text{CO})\text{Cl}$ of which the central Ir(III) atom shows saturated six-coordination mode.^{6-8,32} The presence of a kinetically inert CO ligand bound to the Ir atom reduces the activities of $\text{Ir}(\text{Por})(\text{CO})\text{Cl}$. Through the reaction of a 1:1.2 molar ratio of TCPPCO_2Me and $[\text{Ir}(\text{COD})\text{Cl}]_2$ in 1,2,4-trichlorobenzene at 190°C for 1 day, $\text{Ir}(\text{TCPPCO}_2\text{Me})(\text{CO})\text{Cl}$ can be prepared. To our delight, hydrolysis of $\text{Ir}(\text{TCPPCO}_2\text{Me})(\text{CO})\text{Cl}$ in a solution of KOH led to the formation of $\text{Ir}(\text{TCPP})\text{Cl}$ in which the bound CO was removed (Scheme 2). As a new class of Ir-porphyrins, the coordinatively unsaturated $\text{Ir}(\text{Por})\text{Cl}$ has an potential to exhibit excellent catalytic activities. The absence of CO in $\text{Ir}(\text{TCPP})\text{Cl}$ is evident from the disappearance of $\nu(\text{C}=\text{O})$ in its FT-IR spectrum, whereas the spectrum of $\text{Ir}(\text{TCPPCO}_2\text{Me})(\text{CO})\text{Cl}$ shows this peak ($\sim 2058\text{ cm}^{-1}$) due to the presence of Ir-CO bond (Figure S1).³⁴

Scheme 2. Ir-Porphyrin Ligand Synthesis.



Reaction of ZrCl_4 and $\text{Ir}(\text{TCPP})\text{Cl}$ in the presence of benzoic acid in DMF at 120°C for 48 h yielded red block crystals of $[\text{Zr}_6(\mu_3\text{-O})_8(\text{OH})_5(\text{H}_2\text{O})_7]_2(\text{Ir}(\text{TCPP})\text{Cl})_3 \cdot \text{solvents}$ ($\text{Ir-PMOF-1}(\text{Zr})$). Both of EDS and XPS analyses suggested that the atomic ratio of $\text{Zr} : \text{Ir} : \text{Cl}$ is around 4 : 1 : 1 in $\text{Ir-PMOF-1}(\text{Zr})$ (Figures S2 and S3; Tables S3 and S4). XPS spectrum displayed two intense peaks at 62.4 and 65.4 eV, assignable to $\text{Ir } 4f_{7/2}$ and $\text{Ir } 4f_{5/2}$, respectively, indicative of the +3 valence nature of Ir.³⁵ In the range of 1900-2200 cm^{-1} in its FT-IR spectrum, there is no characteristic peak of the carbonyl stretching, confirming the absence of CO in the axial position of the Ir(III) atom (Figure S4).^{34,35}

Single-crystal X-ray diffraction studies reveal that $\text{Ir-PMOF-1}(\text{Zr})$ crystallizes in cubic space group $Im\bar{3}m$, and is an isostructure of PCN-224.^{28a} Six Zr(IV) atoms connect eight μ_3 -oxygen atoms to form a Zr_6O_8 octahedron cluster, in which

each Zr atom is further occupied by two terminal OH (or H_2O) and each Zr_3 face is capped by a $\mu_3\text{-O}$ atom. As shown in Figure 1a, six edges of the Zr_6 octahedron are bridged by carboxylates from six different 4-connecting $\text{Ir}(\text{TCPP})\text{Cl}$ ligands (Figure 1b), imposing a D_{3d} symmetry to furnish the 3D framework of $\text{Ir-PMOF-1}(\text{Zr})$ (Figure 1c, d), in which the same square-like channels of 1.9×1.9 nm (atom-to-atom distances across opposite Ir metal atoms) intercross in three orthogonal directions. It is worthy to mention that, due to high crystal and molecular symmetry, exactly identifying O^{2-} , OH^- and H_2O groups involved in coordination with Zr_6 cluster is impossible solely depending on the single-crystal analysis, because the statistical nature of the diffraction result averages the distances between difference Zr-O bonds. Nevertheless, based on the chemical compositions and metal charges determined from EDS, XPS and elemental analyses, we speculate a formula of $[\text{Zr}_6(\mu_3\text{-O})_8(\text{OH})_2(\text{H}_2\text{O})_{10}]_2(\text{Ir}(\text{TCPP})\text{Cl})_3$ for the coordination framework, in which the $\mu_3\text{-O}$ oxygen atoms are most probably O^{2-} (Zr-O, 2.058-2.154 Å), while terminal $\mu_1\text{-O}$ oxygen atoms are statistically distributed OH^- and H_2O which are indistinguishable (Zr-O, 2.263 Å). For Ir centers, half of axial positions are vacant while the rest are coordinated by Cl^- anions. The powder X-ray diffraction (PXRD) patterns of bulk samples of $\text{Ir-PMOF-1}(\text{Zr})$ closely match the simulated one from its single-crystal data (Figure S5), indicative of satisfactory phase purity of the product.

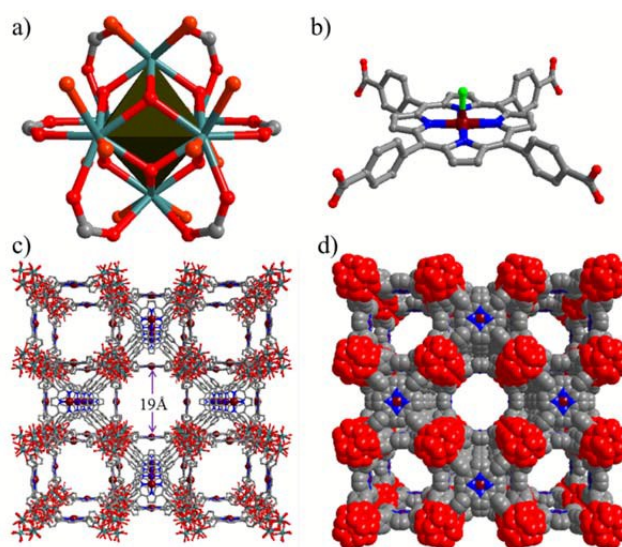


Figure 1. Crystal structures of $\text{Ir-PMOF-1}(\text{Zr})$: (a) the 6-connected Zr_6 cluster; (b) the 4-connected Ir-porphyrin ligand $\text{Ir}(\text{TCPP})\text{Cl}$; (c) and (d) the 3D framework showing open channels (the axial Cl atoms are removed for clarity). Ir (dark red), Zr (teal), N (blue), O (red), Cl (bright green) and C (gray).

It has been discovered that the coordination environment around the Zr_6 cluster could be tuned by adjusting the reactions conditions such as the ratio of Zr(IV) salt to porphyrin ligand and the amount of modulating reagent such as benzoic acid and acetic acid (Table S5).^{13,24,25,28} So far, several typical topology nets containing Zr_6 clusters, including (4,12)-

connected **ftw-a** net in PCN-228^{28c} (or CPM-99¹³, FJI-H6²⁴), (4-8)-connected **csq** net in PCN-222^{28b} (or MOF-545²⁵) and (4,6)-connected **she** net in PCN-224^{28a}, have been constructed based on tetracarboxylated porphyrin ligands. It should be noted that the 12-connected Zr₆ clusters and TCPP ligands are difficult to form **ftw-a** network due to the steric effect between the porphyrin ring and the phenyl ring. Alternatively, the 12-connected Zr₈ clusters behave as the building units in **ftw-a** net as represented in PCN-221,^{28d} or the elongated porphyrinic TCBPP (tetrakis(4-carboxyphenyl)porphyrin) ligands are used to construct **ftw-a** net as in PCN-228 (or CPM-99, FJI-H6). Ir-PMOF-1(Zr) has the same (4,6)-connected topology as PCN-224, and the lower connectivity is resulted from the relatively high ZrCl₄/Ir(TCPP)Cl ratio, i.e. 7.2:1. When this Zr/porphyrin ratio was decreased to 4.4:1, red cubic crystals of Ir-PMOF-2(Zr) were obtained (Table S5). Due to the poor crystal data, its crystal structure couldn't be well refined. Single-crystal study shows that Ir-PMOF-2(Zr) crystallizes in space group *Pm-3m*, and is an isostructure of PCN-221 (Figure S6). It should be noted that Ir-PMOF-2(Zr) has been obtained in much shorter reaction time (8-12 h for Ir-PMOF-2(Zr) vs. 48 h for Ir-PMOF-1(Zr)), which might indicate that Ir-PMOF-2(Zr) was kinetically favoured phase, whereas Ir-PMOF-1(Zr) was thermodynamically favoured phase.

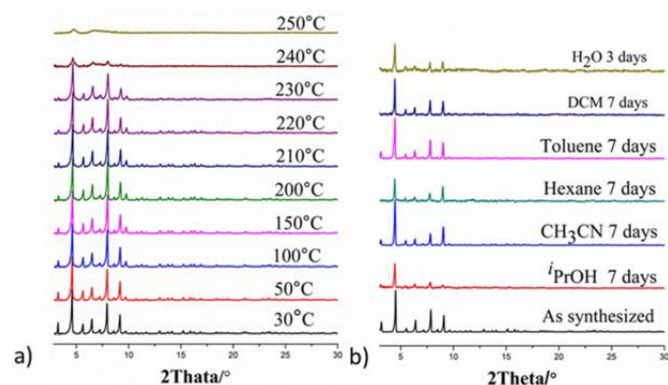


Figure 2. Thermal and chemical stability study of Ir-PMOF-1(Zr): (a) the variable-temperature PXRD patterns from 30 to 250°C; (b) the PXRD patterns upon treatments in different solvents.

Ir-PMOF-1(Zr) crystals exhibit high thermal stability. The thermal gravimetric (TG) curve of the air-dried Ir-PMOF-1(Zr) sample displays a gradual weight loss up to 370°C, indicating that the solvated molecules are evacuated slowly upon heating (Figure S7). The thermal stability of Ir-PMOF-1(Zr) has been further testified by the variable temperature PXRD measurements, indicating that the framework can sustain heating up to 240°C (Figure 2a). Moreover, Ir-PMOF-1(Zr) possesses excellent chemical stability. The PXRD monitoring of the fresh crystals immersed in common organic solvents such as isopropanol (*i*PrOH), acetonitrile (CH₃CN), hexane, toluene, dichloromethane (DCM), and water (H₂O) for several days confirmed that the coordination framework was intact (Figures 2b and S8a-f).

To evaluate the porosity of Ir-PMOF-1(Zr), N₂ adsorption-desorption isotherms at 77 K were measured (Figure 3). Prior to sorption examination, the samples are subjected to solvent exchange with acetone for 5 days and activated by heating at 120 °C under vacuum for 18 h. The N₂ adsorption of Ir-PMOF-1(Zr) shows typical type-I isotherm, in accord with micro-porosity identified by the single-crystal analysis. The N₂ uptake is 705 cm³ g⁻¹ (STP), and the calculated total pore volume is 1.09 cm³ g⁻¹. The Brunauer-Emmet-Teller (BET) surface area is estimated to be 2637 m² g⁻¹, which is comparable with the value of isostructural PCN-224(Ni) (2600 m² g⁻¹).²⁸ The theoretical BET surface and pore volume of Ir-PMOF-1(Zr) are calculated to be 2625 m² g⁻¹ and 1.40 cm³ g⁻¹, respectively, by Materials Studio 6.1.³⁶

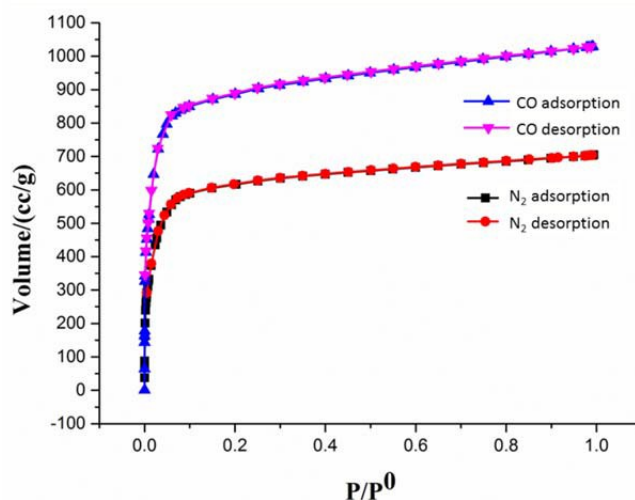


Figure 3. N₂ and CO gas adsorption-desorption isotherms of Ir-PMOF-1(Zr) at 77 K.

Capturing or adsorbing carbon monoxide is of importance due to its high toxicity and poison effect in catalysis and fuel cells. A high affinity to CO was rarely observed for metal-organic materials.³⁷ It has been reported that a rhodium-based MOF DUT-82 (DUT = Dresden University of Technology) has an especially high CO adsorption capability, which can adsorb as high as 800 cm³ g⁻¹ of CO at 77 K (0.59 bar). The CO storage capability of Ir-PMOF-1(Zr) has been examined (Figure 3). At 77 K and 0.57 bar, the CO uptake reaches 1029 cm³ g⁻¹, corresponding to about 73 CO molecules adsorbed per subunit of (Ir(TCPP)Cl).

The transportation ability through the large channels in Ir-PMOF-1(Zr) has been evaluated by the dye uptake test. Two organic dyes, i.e. orange gelb (OG, 15.6 × 10.1 × 5.4 Å³) and methylene blue (MB, 16.3 × 7.9 × 4.0 Å³), are chosen for the adsorption measurements.³⁸ MB and OG have similar size but different charges. MB is a cationic dye, whereas OG is an anionic dye. The adsorption amounts of the dye per gram of Ir-PMOF-1(Zr) for OG and MB are estimated to be 7.2 and 58.4 mg g⁻¹, respectively (Figure S9), suggesting that the large channels (19 × 19 Å²) of Ir-PMOF-1(Zr) are permeable and able to transport bulky organic molecules. The difference in

adsorbed amounts of these two dyes might partly be explained by the acidity of the node –OH and –OH₂ sites.³⁹

The insertion into polar X-H bonds (X = N, O, S) has attracted a lot of interests since Merck's commercial synthesis of the antibiotic thienamycin using dirhodium complex to catalyze the carbenoid insertion into the N-H bonds of β -lactams.⁴⁰ Copper and dirhodium complexes are the most common catalysts, whereas a few other metals (e.g. Fe, Ru, Pd, In, Re) have been occasionally used in X-H insertion reactions.⁴¹ To our surprise, no Ir-based catalysts have been reported in the insertion reaction of a carbene into the O-H bond, while there are two examples of Ir-catalyzed N-H insertions.^{6,42}

To examine the catalytic capability of iridium(III) porphyrins in O-H insertion reactions, a homogeneous catalyst of Ir(TPP)(CO)Cl (TPP = tetraphenylporphyrin) was prepared and then employed in the O-H insertion reaction of isopropanol (*i*PrOH) with ethyl diazoacetate (EDA), where the molar ratio of catalyst : EDA : *i*PrOH is 0.01 : 1 : 5. After the reaction proceeded in DCM at room temperature for 10 min, all of EDA was consumed and the conversion of EDA into alkoxyacetate **2a** was 88% (Table 1, entry 1). Under the similar reaction condition but using dirhodium acetate (Rh₂(OAc)₄) as the catalyst instead of Ir(TPP)(CO)Cl, the conversion of EDA to **2a** was 83% (entry 2). These catalytic results suggest that iridium(III) porphyrins have compatible capability as the acknowledged powerful O-H insertion catalysts, i.e. Rh₂(OAc)₄.

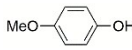
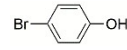
To our delight, the self-supported MOF catalyst Ir-PMOF-1(Zr) can even increase the conversion up to 94% (entry 3) under the heterogeneous reaction condition. In the first 1 min, the conversions into **2a** in the presence of Ir(TPP)(CO)Cl and Ir-PMOF-1(Zr) were 33% and 71%, respectively (entries 4 and 5), indicating the heterogeneous catalyst Ir-PMOF-1(Zr) has an excellent initial rate. The superior activity of Ir-PMOF-1(Zr) may be ascribed to the vacant coordination sites on the axial positions of the central Ir atoms. Moreover, the large and uniform pores of the framework enable each active Ir-site accessible for catalytic purpose. Based on our catalytic results, the turnover frequency (TOF) of Ir-PMOF-1(Zr) is up to 4260 h⁻¹. When decreasing the molar percent of [Ir] to 0.1%, the reaction in the presence of Ir-PMOF-1(Zr) still achieved 77% conversion, although a much longer reaction time of 2.5 h was required (entry 6).

In addition to isopropanol, other alcohols such as methanol and ethanol can take part in the Ir-PMOF-1(Zr) catalyzed O-H insertion reactions, and the alkoxyacetate products **2b** and **2c** are produced with 80% and 87% yields, respectively (Table 1, entries 7 and 8). Phenols are another important group of compounds containing O-H bonds. We have examined the O-H insertion reactions for phenol, 4-methoxyphenol and 4-bromophenol. In the presence of 1 mol [Ir]% of Ir-PMOF-1(Zr), all of EDA was consumed in 10 min, whereas phenoxyacetate products **3a**, **3b** and **3c** were obtained with 56%, 63% and 70% yields, respectively (Table 1, entries 9-11). In addition to the O-H insertion products, the self-coupling reaction products of EDA, i.e. diethyl fumarate and maleate accounted for all initial EDA.

View Article Online

DOI: 10.1039/C6CE00358C

Table 1. Catalytic O-H Insertion.

Entry	Catalyst	Substrate	Product	Yield ^a (%)
1	Ir(TPP)(CO)Cl	<i>i</i> PrOH	2a	88
2	Rh ₂ (OAc) ₄	<i>i</i> PrOH	2a	83
3	Ir-PMOF-1(Zr)	<i>i</i> PrOH	2a	94
4 ^b	Ir(TPP)(CO)Cl	<i>i</i> PrOH	2a	33
5 ^b	Ir-PMOF-1(Zr)	<i>i</i> PrOH	2a	71
6 ^c	Ir-PMOF-1(Zr)	<i>i</i> PrOH	2a	77
7	Ir-PMOF-1(Zr)	MeOH	2b	80
8	Ir-PMOF-1(Zr)	EtOH	2c	87
9	Ir-PMOF-1(Zr)		3a	56
10	Ir-PMOF-1(Zr)		3b	63
11	Ir-PMOF-1(Zr)		3c	70

^aReaction conditions: 1 mol [Ir]% of the catalyst, 10 min. The yields are based on the conversions of EDA to the O-H insertion products. ^bReaction time: 1min. ^cCatalyst amount: 0.1 mol [Ir]%.

The high stability of Ir-PMOF-1(Zr) makes it a robust heterogeneous catalyst. As testified by the PXRD monitoring before and after catalytic reactions (Figure S7), the crystal framework of Ir-PMOF-1(Zr) remains stable after the catalytic reactions. Inductively coupled plasma optical emission spectrometer (ICP-OES) analysis of the reaction filtrate indicated that the amount of the Ir leaching into the reaction mixture was less than 0.06% of the total Ir content in Ir-PMOF-1(Zr). The crystalline catalysts can be easily isolated by centrifugation, and can be reused at least nine times without significant loss of activity (Figure 3). Before each repeating run, Ir-PMOF-1(Zr) catalyst was washed with DCM (3 × 5 mL) to remove the adsorbed organic compounds in the interior and exterior surfaces. During the nine reaction runs, the yields of **2a** were in the range of 88-94%, whereas in the tenth run, the yield was reduced to 64%. To sum up, the turnover number (TON) is up to 875 after ten successive runs (Table S6). The PXRD patterns of the recycled catalyst after the tenth run still show comparable diffraction profile with the as-synthesized sample (Figure S10).

CONCLUSION

In conclusion, we have successfully embedded the versatile homogeneous iridium(III)-porphyrin catalyst into a stable and porous zirconium metal-organic framework, and the resulting

Ir-PMOF-1(Zr) carries coordinatively unsaturated Ir active sites and shows high stability against organic solvents, water, as well as heating (up to 240°C). As a self-supported heterogeneous catalyst, Ir-PMOF-1(Zr) is efficient in O-H insertion reaction of alcohols and phenols, displaying superior capabilities to the related homogenous catalysts. In the reaction system, Ir-PMOF-1(Zr) manifests advantages in easy recycling, reusable catalysis and good stability, thereof implying a promising application by developing and improving such kind of self-supporting heterogeneous catalyst based on iridium(III)-porphyrin metal-organic frameworks.

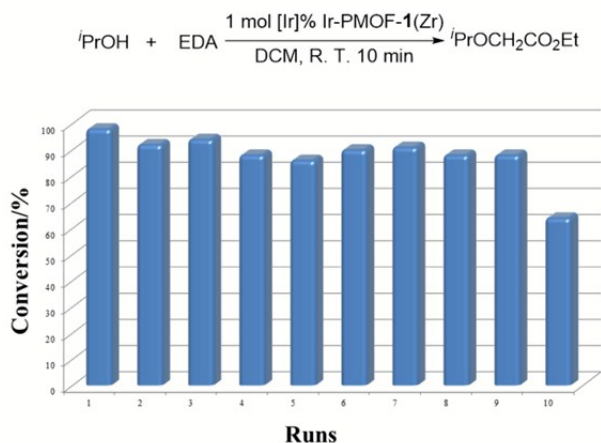


Figure 4. Recycling experiments.

Acknowledgements

This work was supported by the 973 Program (2012CB821701), the NSFC Projects (21373278, 21450110063, 91222201), the STP Project of Guangzhou (15020016), the NSF of Guangdong Province (S2013030013474) and the RFPD of Higher Education of China (20120171130006).

Notes and references.

- J. Ma, L. Zhang, S. Zhu, *Curr. Org. Chem.*, 2016, **20**, 102-118.
- I. Aviv, Z. Gross, *Chem. Commun.*, 2006, 4477-4479.
- S. Zhu, X. Xu, J. A. Perman, X. P. Zhang, *J. Am. Chem. Soc.*, 2010, **132**, 12796-12799.
- C.-M. Ho, J.-L. Zhang, C.-Y. Zhou, O.-Y. Chan, J. J. Yan, F.-Y. Zhang, J.-S. Huang, C.-M. Che, *J. Am. Chem. Soc.*, 2010, **132**, 1886-1894.
- (a) H. J. Callot, F. Metz, C. Piechocki, *Tetrahedron* 1982, **38**, 2365-2369; (b) H.-Y. Thu, G. S.-M. Tong, J.-S. Huang, S. L.-F. Chan, Q.-H. Deng, C.-M. Che, *Angew. Chem. Int. Ed.*, 2008, **47**, 9747-9751.
- B. J. Anding, L. K. Woo, *Organometallics* 2013, **32**, 2599-2607.
- J.-C. Wang, Y. Zhang, Z.-J. Xu, V. K.-Y. Lo, C.-M. Che, *ACS Catal.*, 2013, **3**, 1144-1148.
- I. Rodríguez-García, C. López-Sánchez, M. Álvarez-Corral and M. Muñoz-Dorado, *Synlett*, 2012, **23**, 2469-2472.
- N. U. Day, C. C. Wamser and M. G. Walter, *Polym. Int.*, 2015, **64**, 833-857.
- J. Liu, L. Chen, H. Cui, J. Zhang, L. Zhang and C. Y. Su, *Chem. Soc. Rev.*, 2014, **43**, 6011-6061. DOI: 10.1039/C6CE00358C
- B. J. Burnett, P. M. Barron, C. Hu, W. Choe, *J. Am. Chem. Soc.*, 2011, **133**, 9984-9987.
- Z. Zhang, L. Zhang, L. Wojtas, M. Eddaoudi, M. J. Zaworotko, *J. Am. Chem. Soc.*, 2012, **134**, 928-933.
- Q. Lin, X. Bu, A. Kong, C. Mao, X. Zhao, F. Bu, P. Feng, *J. Am. Chem. Soc.*, 2015, **137**, 2235-2238.
- A. Fateeva, S. Devautour-Vinot, N. Heymans, T. Devic, J.-M. Grenèche, S. Wuttke, S. Miller, A. Lago, C. Serre, G. De Weireld, G. Maurin, A. Vimont, G. Férey, *Chem. Mater.*, 2011, **23**, 4641-4651.
- G. Nandi, I. Goldberg, *Chem. Commun.*, 2014, **50**, 13612-13615.
- I. Hod, M. D. Sampson, P. Deria, C. P. Kubiak, O. K. Farha, J. T. Hupp, *ACS Catal.*, 2015, **5**, 6302-6309.
- H.-C. Kim, Y. S. Lee, S. Huh, S. J. Lee, Y. Kim, *Dalton Trans.*, 2014, **43**, 5680-5686.
- L. Meng, Q. Cheng, C. Kim, W.-Y. Gao, L. Wojtas, Y.-S. Chen, M. J. Zaworotko, X. P. Zhang, S. Q. Ma, *Angew. Chem. Int. Ed.*, 2012, **51**, 10082-10085.
- S. R. Ahrenholtz, C. C. Epley, A. J. Morris, *J. Am. Chem. Soc.*, 2014, **136**, 2464-2472.
- A. Fateeva, P. A. Chater, C. P. Ireland, A. A. Tahir, Y. Z. Khimyak, P. V. Wiper, J. R. Darwent, M. J. Rosseinsky, *Angew. Chem. Int. Ed.*, 2012, **51**, 7440-7444.
- E. A. Dolgoplova, D. E. Williams, A. B. Greytak, A. M. Rice, M. D. Smith, J. A. Krause, N. B. Shustova, *Angew. Chem. Int. Ed.*, 2015, **54**, 13639-13643.
- K. S. Suslick, P. Bhyrappa, J. -H. Chou, M. E. Kosal, S. Nakagaki, D. W. Smithenry, S. R. Wilson, *Acc. Chem. Res.*, 2005, **38**, 283-291.
- C. Zou, Z. Zhang, X. Xu, Q. Gong, J. Li, C.-D. Wu, *J. Am. Chem. Soc.*, 2012, **134**, 87-90.
- J. Zheng, M. Wu, F. Jiang, W. Su, M. Hong, *Chem. Sci.*, 2015, **6**, 3466-3470.
- W. Morris, B. Voloskiy, S. Demir, F. Gándan, P. L. McGrier, H. Furukawa, D. Cascio, J. F. Stoddart, O. M. Yaghi, *J. Am. Chem. Soc.*, 2015, **137**, 2199-2202.
- N. Kornienko, Y. Zhao, C. S. Kley, C. Zhu, D. Kim, S. Lin, C. J. Chang, O. M. Yaghi, P. Yang, *J. Am. Chem. Soc.*, 2015, **137**, 14129-14135.
- J. A. Johnson, X. Zhang, T. C. Reeson, Y.-S. Chen, J. Zhang, *J. Am. Chem. Soc.*, 2014, **136**, 15881-15884.
- (a) D. Feng, W.-C. Chung, Z. Wei, Z.-Y. Gu, H.-L. Jiang, Y.-P. Chen, D. J. Darensbourg, H.-C. Zhou, *J. Am. Chem. Soc.*, 2013, **135**, 17105-17110. (b) D. Feng, Z.-Y. Gu, J.-R. Li, H.-L. Jiang, Z. Wei, H.-C. Zhou, *Angew. Chem. Int. Ed.*, 2012, **51**, 10307-10310. (c) T.-F. Liu, D. Feng, Y.-P. Chen, L. Zou, M. Bosch, S. Yuan, Z. Wei, S. Fordham, K. Wang, H.-C. Zhou, *J. Am. Chem. Soc.*, 2015, **137**, 413-419. (d) D. Feng, H.-L. Jiang, Y.-P. Chen, Z.-Y. Gu, Z. Wei, H.-C. Zhou, *Inorg. Chem.* 2013, **52**, 12661-12667.
- D. Hagrman, P. J. Hagrman, J. Zubieta, *Angew. Chem. Int. Ed.*, 1999, **38**, 3165-3168.
- J. Kang, B. Zhu, J. Liu, B. Wang, L. Zhang, C.-Y. Su, *Org. Chem. Front.*, 2015, **2**, 890-907.
- (a) L. Chen, J. Kang, H. Cui, X. Wang, L. Liu, L. Zhang, C.-Y. Su, *Dalton Trans.*, 2015, **44**, 12180-12188. (b) L. Chen, T. Yang, H. Cui, T. Cai, L. Zhang, C.-Y. Su, *J. Mater. Chem. A* 2015, **3**, 20201-20209.
- (a) H. Ogoshi, J.-I. Setsune, Z.-I. Yoshida, *J. Organomet. Chem.* 1978, **159**, 317-328. (b) K. J. Del Rossi, B. B. Wayland, *J. Chem. Soc., Chem. Commun.* 1986, 1653-1655. (c) S. K. Yeung, K. S. Chan, *Organometallics* 2005, **24**, 6426-6430.
- (a) O.V. Dolomanov, L.J. Bourhis, R.J. Gildea, J.A.K. Howard, H. Puschmann, *J. Appl. Cryst.*, 2009, **42**, 339-341; (b) L. J. Farrugia, *J. Appl. Cryst.*, 1999, **32**, 837-838; (c) P. V. D. Sluis,

- A. L. Spek, *Acta Cryst., Sect. A: Found. Crystallogr.*, 1990, **46**, 194-201.
- 34 J. L. Cornillon, J. E. Anderson, C. Swistak, K. M. Kadish, *J. Am. Chem. Soc.*, 1986, **108**, 7633-7640.
- 35 T. V. Voskoboynikov, E. S. Shpiro, H. Landmesser, N. I. Jaeger and G. Schulz-Ekloff, *J. Mol. Catal. A-Chem.*, 1996, **104**, 299-309.
- 36 T. Düren, F. Millange, G. Férey, K. S. Walton and R. Q. Snurr, *J. Phys. Chem. C*, 2007, **111**, 15350-15356.
- 37 G. Nickerl, U. Stoeck, U. Burkhardt, I. Senkovska and S. Kaskel, *J. Mater. Chem. A*, 2014, **2**, 144-148.
- 38 X. Zhao, X. Bu, T. Wu, S. T. Zheng, L. Wang and P. Feng, *Nat Commun.*, 2013, **4**, 2344.
- 39 R. C. Klet, S. Tussupbayev, J. Borycz, J. R. Gallagher, M. M. Stalzer, J. T. Miller, L.; Gagliardi, J. T. Hupp, T. J. Marks, C. J. Cramers, M. Delferro, O. K. Farha, *J. Am. Chem. Soc.*, 2015, **137**, 15680-15683.
- 40 T. N. Salzmann, R. W. Ratcliffe, B. G. Christensen and F. A. Bouffard, *J. Am. Chem. Soc.*, 1980, **102**, 6161-6163.
- 41 A. Ford, H. Miel, A. Ring, C. N. Slattery, A. R. Maguire and M. A. McKervey, *Chem Rev*, 2015, **115**, 9981-10080.
- 42 I. K. Mangion, I. K. Nwamba, M. Shevlin and M. A. Huffman, *Org. Lett.*, 2009, **11**, 3566-3569.

View Article Online
DOI: 10.1039/C6CE00358C